Crystal Structures of RIα Subunit of Cyclic Adenosine 5′-Monophosphate (cAMP)-Dependent Protein Kinase Complexed with (R_p)-Adenosine 3′,5′-Cyclic Monophosphothioate and (S_p)-Adenosine 3′,5′-Cyclic Monophosphothioate, the Phosphothioate Analogues of cAMP[†,‡]

Jian Wu,[§] John M. Jones,[⊥] Nguyen-Huu Xuong,[§,∥] Lynn F. Ten Eyck,[§,▽] and Susan S. Taylor*[,§,⊥]

Department of Chemistry and Biochemistry, University of California, San Diego, La Jolla, California 92093, Howard Hughes Medical Institute, University of California, San Diego, La Jolla, California 92093, Department of Biology and Physics, University of California, San Diego, La Jolla, California 92093, and San Diego Supercomputer Center, San Diego, California 92186

Received November 30, 2003; Revised Manuscript Received March 23, 2004

ABSTRACT: Cyclic adenosine 5′-monophosphate (cAMP) is an ancient signaling molecule, and in vertebrates, a primary target for cAMP is cAMP-dependent protein kinase (PKA). (R_p)-adenosine 3′,5′-cyclic monophosphothioate ((R_p)-cAMPS) and its analogues are the only known competitive inhibitors and antagonists for cAMP activation of PKA, while (S_p)-adenosine 3′,5′-cyclic monophosphothioate ((S_p)-cAMPS) functions as an agonist. The crystal structures of a Δ(1−91) deletion mutant of the RIα regulatory subunit of PKA bound to (R_p)-cAMPS and (S_p)-cAMPS were determined at 2.4 and 2.3 Å resolution, respectively. While the structures are similar to each other and to the crystal structure of RIα bound to cAMP, differences in the dynamical properties of the protein when (R_p)-cAMPS is bound are apparent. The structures highlight the critical importance of the exocyclic oxygen's interaction with the invariant arginine in the phosphate binding cassette (PBC) and the importance of this interaction for the dynamical properties of the interactions that radiate out from the PBC. The conformations of the phosphate binding cassettes containing two invariant arginine residues (Arg209 on domain A, and Arg333 on domain B) are somewhat different due to the sulfur interacting with this arginine. Furthermore, the B-site ligand together with the entire domain B show significant differences in their overall dynamic properties in the crystal structure of Δ(1−91) RIα complexed with (R_p)-cAMPS phosphothioate analogue ((R_p)−RIα) compared to the cAMP- and (S_p)-cAMPS-bound type I and II regulatory subunits, based on the temperature factors. In all structures, two structural solvent molecules exist within the A-site ligand binding pocket; both mediate water-bridged interactions between the ligand and the protein. No structured waters are in the B-site pocket. Owing to the higher resolution data, the N-terminal segment (109−117) of the RIα subunit can also be traced. This strand forms an intermolecular antiparallel β-sheet with the same strand in an adjacent molecule and implies that the RIα subunit can form a weak homodimer even in the absence of its dimerization domain.

Cyclic adenosine 5′-monophosphate (cAMP)[1] acts as a major second messenger in a multitude of cellular processes to convert an extracellular event into a biological response. Several diseases are associated with unusually high or low levels of cAMP and with disruptions in this cAMP-mediated signaling pathway. In bacteria, cAMP regulates gene expression through binding to a catabolite repressor protein (CAP) (*1*). In eukaryotic cells, the primary receptors for cAMP are the regulatory subunits (R) of cAMP-dependent protein kinase (PKA) (*2*, *3*). Other mammalian receptors for cAMP that utilize the same cAMP binding motif include the cyclic nucleotide-gated channels (*4*) and the guanine nucleotide exchange protein (EPAC) (*5*, *6*).

Despite the presence of other cyclic nucleotide binding proteins, the two major forms of PKA, type I and II, are ubiquitous in mammalian cells and are thought to mediate most known biological effects of cAMP (*7*, *8*). The regulatory subunits of isozymes I and II, referred to as RI and RII, are functionally distinct and are further subclassified into α- and β-forms, leading to four distinct R-subunits (RIα,

[†] This work was supported by a grant from the National Institutes of Health (Grant GM 34921) to S. S. Taylor.

[‡] The coordinates of (R_p)−RIα and (S_p)−RIα are deposited in the Protein Data Bank with accession codes of 1NE4 and 1NE6.

* To whom correspondence should be addressed. Mailing address: Howard Hughes Medical Institute, Department of Chemistry and Biochemistry, University of California, San Diego, 9500 Gilman Drive, CMM West 105, La Jolla, CA 92093-0654. Telephone: (858)-534−3677. Fax: (858)-534-8193. E-mail: staylor@ucsd.edu.

[§] Department of Chemistry and Biochemistry, UCSD.

[⊥] Howard Hughes Medical Institute, UCSD.

[∥] Department of Biology and Physics, UCSD.

[▽] San Diego Supercomputer Center.

[1] Abbreviations: cAMP, cyclic adenosine 5′-monophosphate; (R_p)-cAMPS, (R_p)-adenosine 3′,5′-cyclic monophosphothioate; (S_p)-cAMPS, (S_p)-adenosine 3′,5′-cyclic monophosphothioate; PKA, cAMP-dependent protein kinase; CAP, catabolite repressor protein; EPAC, guanine nucleotide exchange protein; R, regulatory subunit; C, catalytic subunit; PBC, phosphate binding cassette.

10.1021/bi0302503 CCC: $27.50
Published on Web 05/05/2004

RIβ, RIIα, and RIIβ), which are the products of separate genes (*9*). All R-subunits share a similar domain organization, which consists of a dimerization/docking domain at the amino terminus, two tandem cAMP binding domains designated as A and B at the carboxyl terminus, and a variable connecting linker region. The linker region contains a substrate-like inhibitor peptide that binds to the active site of the catalytic subunit (C). The two cAMP binding domains A and B are similar in their primary amino acid sequence (*10*) but differ with respect to their cAMP analogue selectivity (*11*) and overall cAMP binding kinetics (*3*). Several criteria distinguish these two sites. Site A has a preference for N6-substituted cAMP analogues and has a faster off-rate for [^{3}H]cAMP, while site B preferentially binds C2- and C8-substituted cAMP analogues and shows a slower off-rate (*12*, *13*). Based on kinetic evidence, PKA mutants (*14*−*16*), and cAMP analogue studies (*17*), the best model indicates that the RIα site A provides the major contact with the C-subunit, while site B is more accessible in the holoenzyme complex than site A. Since cAMP binding is highly cooperative (*18*, *19*), it is predicted that the binding of cAMP to site B induces a conformational change that makes site A more accessible to cAMP. The subsequent occupation of site A by cAMP causes dissociation of the wild-type holoenzyme. The crystal structures of a Δ(1−91) deletion mutant of RIα (*20*) and the Δ(1−111) deletion mutant of RIIβ (*21*) with cAMP complexed to both sites reveal the conserved architecture of the two cAMP-binding sites as well as structural details of key residues involved in cAMP binding. These structures also provide the molecular basis for understanding how cAMP binds cooperatively to isozymes I and II of PKA, thus promoting signaling to different target proteins. The structural analysis indicates that the exocyclic equatorial oxygens of cAMP interact with the guanidinium side chains of an invariant arginine residue at positions 209 (domain A) and 333 (domain B) for the RIα subunit and positions 230 (domain A) and 359 (domain B) for the RIIβ subunit. This invariant arginine is a key feature of the cAMP phosphate binding cassette (PBC). Earlier data based on cAMP analogue mapping studies and site-directed mutagenesis also support and explain the importance of these arginine residues for cAMP binding (*15*, *16*).

Until recently, PKA represented a main target protein for the development of cyclic nucleotide analogues that might be prospective drugs or tools for biochemical and pharmacological studies. A cAMP analogue was recently identified that shows specificity for EPAC (*22*). Over the past four decades, hundreds of cAMP analogues have been synthesized and investigated for their therapeutic potential. These analogues have provided considerable information about specificity requirements for kinase activation and several show high preference for isoform-specific domains (*23*). However, (R_p)-cAMPS ((R_p)-adenosine 3′,5′-cyclic monophosphothioate) and its adenine-base modified derivatives are the only known analogues of cAMP that act as competitive inhibitors and antagonists of cAMP-induced activation of PKA. The corresponding diasteriomeric (S_p)-cAMPS analogues (Figure 1) are agonists (*24*, *25*). (R_p)-cAMPS has a single sulfur substitution for the exocyclic equatorial oxygen, whereas the exocyclic axial position of the cyclophosphate ring is substituted in (S_p)-cAMPS. The introduction of sulfur for the exocyclic oxygen results in a substantial decrease in binding affinity. The affinity determination of a set of doubly modified (R_p)- or (S_p)-analogues shows that (S_p) isomers have a 5-fold lower affinity for site A and a 30-fold lower affinity for site B of the RIα subunit. The mean reduction in affinity for the (R_p) isomers are approximately 400-fold and 200-fold for site A and B, respectively (*26*). Previous studies have demonstrated that the antagonists bind to both type I and type II holoenzymes but keep the protein in a locked conformation, thus preventing activation of the holoenzymes (*27*, *28*).

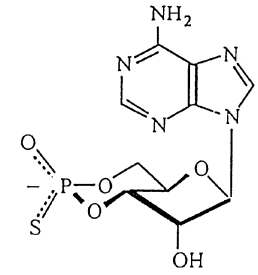

Rp-cAMP

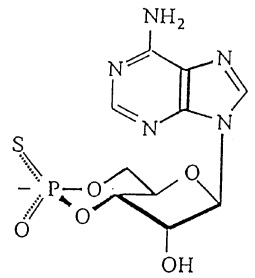

Sp-cAMP

FIGURE 1: Chemical structures of (R_p)-cAMPS and (S_p)-cAMPS phosphothioate analogues.

(R_p)-cAMPS differs from cAMP and (S_p)-cAMPS only in the exocyclic substitution but shows the opposite biological response when bound to the regulatory subunit of PKA. To determine the molecular basis for the antagonistic properties of (R_p)-cAMPS and to establish why the (R_p)-cAMPS phosphothioate analogue can keep the protein in the holoenzyme conformation (H-form), while cAMP and (S_p)-cAMPS dissociate the holoenzyme by switching to the cAMP-bound conformation (B-form), we crystallize Δ(1−91) RIα with (R_p)-cAMPS and (S_p)-cAMPS, respectively. The crystal structures of Δ(1−91) RIα complexed with (R_p)-cAMPS phosphothioate analogue ((R_p)−RIα) and the corresponding (S_p)-cAMPS analogue ((S_p)−RIα) are compared to the structure of Δ(1−91) RIα bound to cAMP (cAMP−RIα). The structures highlight the critical importance of the interaction of the exocyclic oxygen with the invariant arginine in the PBC and the importance of this interaction for the dynamical properties of the allosteric interactions that radiate out from the PBC.

MATERIALS AND METHODS

Preparation of (R_p)−RIα and (S_p)−RIα proteins. The recombinant Δ(1−91) deletion mutant of RIα was expressed and purified by affinity chromatography as described previously (*29*). An improvement was achieved by eluting from the cAMP affinity resin with cGMP instead of cAMP. The cGMP-eluted protein behaves like the stripped regulatory

Table 1: Crystal Data and Data Collection Statistics

	(R_p)−RIα	(S_p)−RIα
space group	$P6_522$	$P6_522$
cell dimensions		
a, *b* (Å)	86.9	87.4
c (Å)	179.0	178.7
no. of molecules per asymmetric unit	1	1
mosaicity	0.33	0.16
resolution range (Å)	50.0−2.4	50.0−2.3
no. of unique reflections	16251	18563
R_{sym} (%)[a]	4.8 (47.3)[b]	4.5 (45.1)
data completeness (%)	99.3 (97.9)	99.5 (97.9)

[a] $R_{sym} = \sum|(I - \langle I\rangle)|/\sum I$. [b] The numbers in the parentheses correspond to the data in the highest resolution shell.

Table 2: Refinement Statistics

	(R_p)−RIα	(S_p)−RIα
no. of amino acid residues	268	268
no. of cAMP analogues	2	2
no. of solvent molecules	93	103
R-factor (%)	20.9	21.1
R_{free} (%)	25.3	24.1
rms[a] deviation from ideality		
bond lengths (Å)	0.007	0.007
bond angles (deg)	1.40	1.43
Ramachandran angles		
disallowed (%)	0.0	0.0
most favored (%)	82.2	83.5

[a] Root-mean-square.

subunit in terms of its thermostability. The cGMP can be readily dialyzed away, in contrast to cAMP. To obtain cAMP-free Δ(1−91) RIα, the purified cGMP-eluted RIα subunits were dialyzed overnight against 200 mM NaCl, 2 mM EDTA, 2 mM EGTA, 10 mM DTT, and 50 mM MES buffer at pH 7.5. After cGMP was removed, the proteins were concentrated and bound to the cAMP analogues using a 10-fold excess of (R_p)-cAMPS or (S_p)-cAMPS, respectively. The (R_p) and (S_p) analogues were purchased from Sigma.

Crystallization and Data Collection. Single crystals of both (R_p)−RIα and (S_p)−RIα were grown in hanging drops using the vapor diffusion method by mixing 2 μl of the protein solution (12 mg ml^{-1}) and 2 μl of the reservoir solution (1.0 M NH_2SO_4, 12.5% glycerol, 10 mM DTT, 0.1 M NaAc buffer, pH 5.5) at 22.5 °C. The crystallization conditions were similar to those used for cAMP−RIα protein (*20*). The crystals grew to 1.0 mm × 0.2 mm × 0.2 mm within a week. The crystals belong to the hexagonal space group $P6_522$ ($P6_122$) with cell dimensions of $a = b = 86.9$ Å, $c = 179.0$ Å for (R_p)−RIα and $a = b = 87.4$ Å, $c = 178.7$ Å for (S_p)−RIα with one molecule in the asymmetric unit, respectively. The crystal data are summarized in Table 1.

The X-ray diffraction data for (R_p)−RIα and (S_p)−RIα crystals were collected initially with a Mar Research Imaging Plate 345 detector system at University of California, San Diego. The crystals diffracted to 2.9 Å resolution. Higher resolution diffraction data (2.4 Å for (R_p)−RIα and 2.3 Å for (S_p)−RIα) were collected on a MAR image plate scanner at the Stanford Synchrotron Radiation Laboratory (SSRL) under cryo conditions at 100 K. Data were processed using DENZO and scaled with SCALEPACK (*30*). The data for (R_p)−RIα was 99.3% complete with an R_{sym} of 4.8% and 99.5% complete with an R_{sym} of 4.5% for (S_p)−RIα. Data collection statistics are also summarized in Table 1.

Structure Refinement. The structure determination and refinement for (R_p)−RIα and (S_p)−RIα were carried out using the program package CNS (*31*) on a Silicon Graphics O2 workstation. Five percent of the data were randomly selected as the test data set used for cross validation. Model building was performed using the graphics software TURBO−FRODO (*32*).

Phases for (R_p)−RIα and (S_p)−RIα successively were generated by applying a difference Fourier method based on the crystal structure of cAMP−RIα at 2.8 Å resolution (*20*), in which two cAMP ligands were omitted. Rigid body refinement was carried out, leading to an *R* factor of 27.4% at 2.8 Å resolution. The structure was then refined for both simulated annealing from 2500 °C and individual *B*-factor for a number of rounds using CNS protocols. During the refinement, the ($2F_o - F_c$) and ($F_o - F_c$) electron density maps were regularly calculated and used for manually rebuilding the model. Simulated annealing "omit" maps were calculated as well when necessary. When the resolution was gradually extended up to 2.4 Å, water molecules were gradually fitted into the model. In the late stage, only those water molecules with reasonable temperature factors that hydrogen bonded directly to protein atoms or through other water molecules were included in the final model. The refinement data are summarized in Table 2.

RESULTS

Structure Determination. To avoid the model bias possibly introduced during the refinement, the structures of (R_p)−RIα and (S_p)−RIα successively were solved from the model of cAMP−RIα, respectively, although the refined (R_p)−RIα structure at 2.4 Å resolution seems to be a good initial model for (S_p)−RIα refinement. Although phase solutions were performed using either $P6_522$ or $P6_122$ as the space group for (R_p)−RIα and (S_p)−RIα crystals, the *R* factors and R_{free} were significantly lower for a solution in $P6_522$ space group.

The final structure of (R_p)−RIα refined at 2.4 Å resolution gave an *R* factor of 20.9% and R_{free} of 25.3%, and refined bond lengths have a root-mean-square deviation of 0.007 Å from ideality, and the bond angles deviate by 1.40°. The *R* factor and R_{free} of the 2.3 Å (S_p)−RIα structure are 21.1% and 24.1%, respectively, while the rms deviations of the bond lengths and bond angles from the ideal values are 0.007 Å and 1.43° (Table 2). Ramachandran plots of the two structures obtained using the program PROCHECK (*33*) show that all of the nonglycine residues are located in the allowed regions with 82.2% for (R_p)−RIα and 83.5% for (S_p)−RIα in the most favored regions.

The final models consist of 268 amino acid residues (109−376), two cAMP-analogue molecules and 93 or 103 water atoms for (R_p)−RIα and (S_p)−RIα, respectively. The ($2F_o - F_c$) and ($F_o - F_c$) electron density of (R_p)-cAMPS and (S_p)-cAMPS analogues in the A-sites are shown in Figure 2, parts a and c, respectively, and indicate the well-defined positions for the two analogues. To help discriminate the (R_p)-cAMPS and (S_p)-cAMPS compared to cAMP, we modeled the electron densities by replacing an oxygen atom into the exocyclic sulfur position in (R_p)−RIα (Figure 2b) and the equatorial sulfur position in the (S_p)−RIα structure (Figure 2d). This revealed extra ($F_o - F_c$) electron density

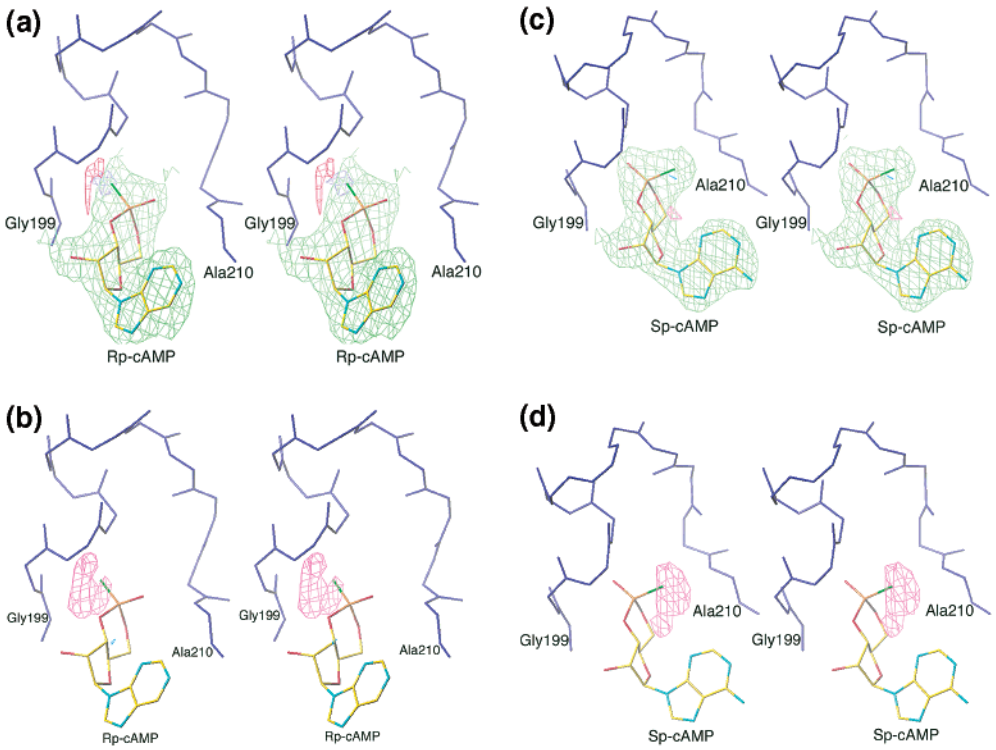

FIGURE 2: Stereoviews of electron density maps. Panels a and c present the $(2F_o - F_c)$ and $(F_o - F_c)$ maps of (R_p)-cAMPS and (S_p)-cAMPS analogues in the A-sites, respectively. The $(2F_o - F_c)$ maps are contoured at 1.5σ (in light green) and the $(F_o - F_c)$ maps at $+3\sigma$ (in red) and -3σ (in blue). The two analogue molecules are shown in atom-type colors with the sulfur atoms in green. The backbone traces of the PBC motifs are also shown. Panels b and d present the $(F_o - F_c)$ maps of (R_p)-cAMPS and (S_p)-cAMPS analogues, respectively, in the A-sites where their sulfur atoms are replaced by oxygen atoms. The densities are contoured at $+3\sigma$ and shown in red. The $(2F_o - F_c)$ maps show no differences during the modeling.

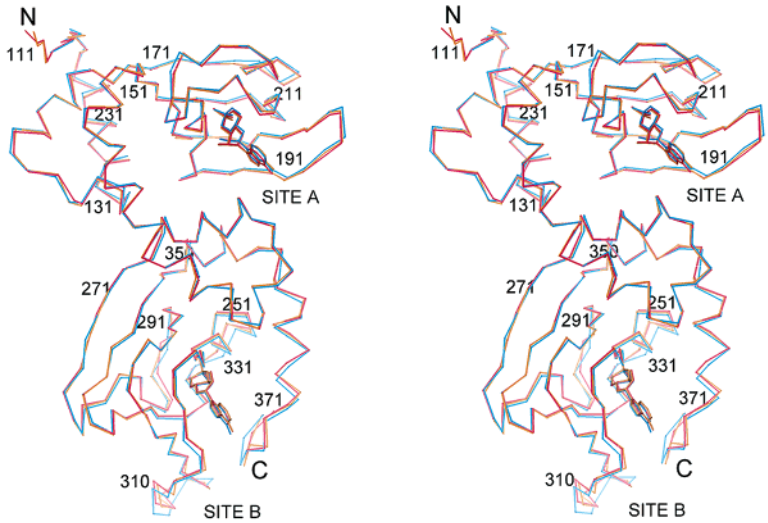

FIGURE 3: Stereoview of Cα backbone and the ligands of (R_p)−RIα superimposed with those of (S_p)−RIα and cAMP−RIα. (R_p)−RIα is shown in red, (S_p)−RIα in golden, and cAMP−RIα in blue. N- and C-termini are indicated. Some residue numbers are labeled to help following the Cα trace.

at the appropriate position containing the position of the sulfur and confirming also that no cAMP was present. The N-terminal segment 94−108 and the C-terminal residues 377−379 could not be traced owing to the lack of well-defined electron density in the $(2F_o - F_c)$ and $(F_o - F_c)$ maps. However, the N-terminus of the newly refined structures showed significant improvement, compared to the earlier structure of cAMP−RIα. Four additional residues (109−112) and all the side chains of the residues of 113−116 could be visualized. A loop region (303−308), located on the molecular surface connecting β4 and β5 of domain B, had high temperature factors, and only the main chain conformation could be traced.

Overall Structures. The overall structures of (R_p)−RIα and (S_p)−RIα are very similar to each other with an rms difference of 0.34 Å for all Cα atoms. The overall structures of these two molecules are also similar to that of cAMP-bound RIα, as shown in Figure 3. The rms deviations of a total of 264 Cα atoms are 0.51 Å between (R_p)−RIα and cAMP−RIα and 0.48 Å between (S_p)−RIα and cAMP−RIα molecules. In addition to the N- and C-terminal regions, some slight conformational differences in the backbone can

be observed in several loop regions in the (R_p)−RIα, (S_p)−RIα, and cAMP−RIα structures. These regions are all solvent-exposed. The most significant change appears at the surface loop region between β4 and β5, residue 303−310 (Figure 3). As mentioned above, only the main chain conformation of this loop can be traced, and the *B* factors are relatively higher than the other regions, suggesting that this segment is somewhat flexible.

Each cAMP-binding domain of the RIα subunit consists of three α-helices and eight β-strands, which form a flattened β barrel surrounding two cAMP ligands. The secondary structures of (R_p)−RIα and (S_p)−RIα are the same as that of cAMP−RIα, especially the helices and the β-sheet surrounding the cAMP binding sites. The most notable feature of the (R_p)−RIα and (S_p)−RIα structures in terms of their secondary structure relates to their N-terminal segments. After including four more residues (109−112) at the N-terminus in both final structures, this segment, residues (109−117), is found to interact with the same N-terminal segment of a symmetry-related molecule, forming an intermolecular antiparallel β-sheet. This β-sheet allows two RIα monomers to pack together as an R homodimer. The structural alignment of (R_p)−RIα, (S_p)−RIα, and cAMP−RIα show some small main- and side-chain conformational changes in the peptide segments that surround the two invariant arginine residues, Arg209 of domain A and Arg333 of domain B in the phosphate binding cassette, although the secondary and tertiary structures of these cAMP binding pockets are basically identical in the three structures. These changes will be described subsequently in the ligand binding section.

There are several solvent-rich regions in the structures of the (R_p) and (S_p) analogues bound to the RIα subunit. Solvent molecules were not included in the original crystal structure of cAMP−RIα due to the lower resolution of the data (*20*). About 15 crystallographic water atoms, in both (R_p)−RIα and (S_p)−RIα, are observed within the A/B domain interfacial crevice, which is formed by helix C and β-strand 5 of domain A, and helix A and helix B of domain B, as well as some loop regions between these elements of secondary structure. The cAMP in domain A can be accessed by this solvated interface. The second solvent-rich region locates at a surface patch on domain A consisting of β-strands 2, 4, and 5 with 10 water atoms in (R_p)−RIα structure. There are also some water molecules (about 14 in both structures) that cluster on the solvent-exposed surface region of helix B and the N-terminus of helix C in domain A. This region is thought to be the catalytic subunit docking surface. In the (R_p)−RIα structure, most of solvent molecules exist at the interface between domain A and domain B, while more solvent molecules appear in domain B in the (S_p)−RIα structure relative to the (R_p)−RIα structure. The most significant structural water molecule, discussed below, is found at the base of the PBC in domain A where it is anchored by the conserved Arg209.

cAMP Analogue Binding Sites. Each cAMP-binding site shows the conserved structural features that are characteristic of this motif, as evidenced by the similarity of each site's hydrogen bonding pattern elucidated from analyses of the (R_p)- and (S_p)-phosphothioate analogues bound to RIα and the cAMP−RIα structures. The phosphate group and the ribose ring both make direct and water-bridged interactions

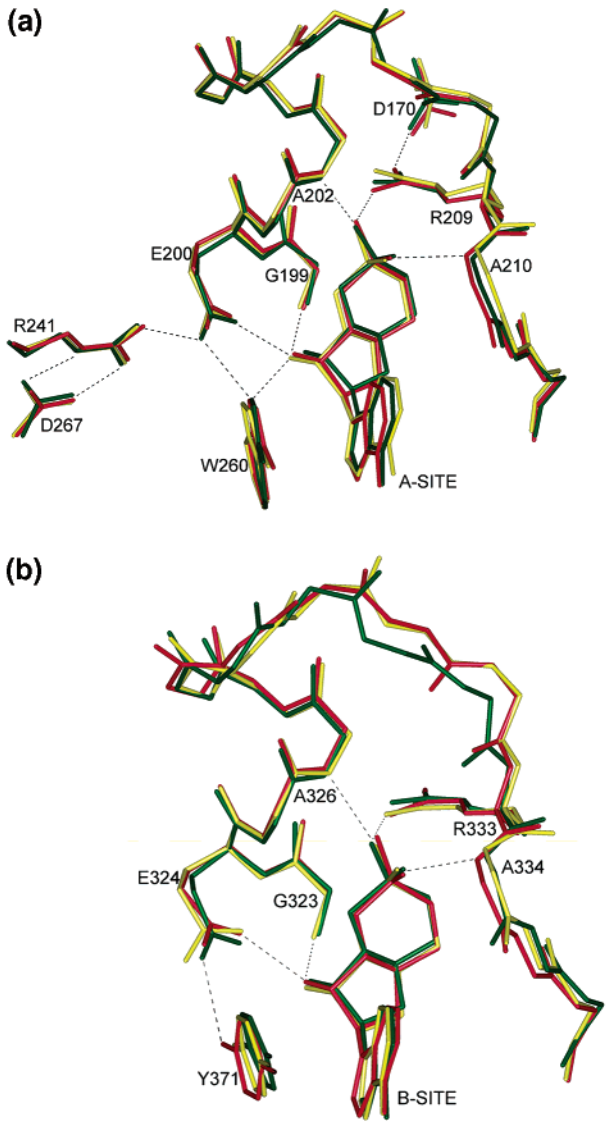

FIGURE 4: The PBC motif and the ligand of (R_p)−RIα within the (a) A-site and (b) B-site superimposed with those of (S_p)−RIα and cAMP−RIα. (R_p)−RIα is shown in red, (S_p)−RIα in yellow, and cAMP−RIα in dark green. The conserved residues in both binding sites are shown. The hydrogen bonds are indicated by dashed lines.

with the protein through several hydrogen bonds and electrostatic contacts. However, there are no direct hydrogen-bonding interactions between the adenine ring and the protein. Most of the interactions with cAMP involve a highly conserved peptide between β-strands 6 and 7, which is referred as the "phosphate binding cassette" or PBC (*21*). The PBC, comprised of residues Gly199−Ala211 in domain A and Gly323−Ala335 in domain B, makes multiple contacts with the phosphate and ribose moieties of cAMP and also with a structural water molecule. Figure 4 shows the PBC motifs of (R_p)−RIα and (S_p)−RIα structures superimposed with that of cAMP−RIα. The interaction patterns of all these direct contacts between the ligand and protein are conserved whether the PBC motif is bound to cAMP or to the (R_p)- and (S_p)-analogues. However, the strength of some of interactions, as indicated by the bond distance, are significantly different for (R_p)−RIα compared to cAMP−RIα and (S_p)−RIα. For example, the distance between the exocyclic equatorial sulfur (S1P) and the NH1 atom of the invariant residue Arg209 is 2.6 Å in the (R_p)−RIα structure. In

Table 3: Direct Contacts between the Ligand and Protein and Hydrogen Bond Interactions of the Solvent Network

(a) Direct Contacts between the Ligand and Protein in (R_p)−, (S_p)−, and cAMP−RIα

atom 1	atom 2	distance (Å)		
		(R_p)−RIα	(S_p)−RIα	cAMP−RIα
		A-Site		
CMP401 S1P (O1P)[a,b]	Arg209 NH1	2.6	3.1	3.2
CMP401 S1P (O1P)	Ala202 N	2.7	2.9	2.6
CMP401 S1P (O1P)	Gly199 O	3.3	3.5	3.6
CMP401 O2P (S2P)	Ala210 N	2.8	3.4	2.9
CMP401 O2′	Gly199 N	2.9	3.0	2.7
CMP401 O2′	Glu200 OE1	2.6	2.6	2.8
CMP401 O2′	Trp260 NE1	3.2	3.3	3.7
Arg209 NH1	Gly199 O	2.8	3.3	3.5
		B-Site		
CMP601 S1P (O1P)	Arg333 NH1	3.1	2.8	3.2
CMP601 S1P (O1P)	Ala326 N	2.9	3.0	2.9
CMP601 S1P (O1P)	Gly323 O	3.5	3.3	3.7
CMP601 O2P (S2P)	Ala334 N	2.6	3.0	2.8
CMP601 O2′	Gly323 N	3.0	2.8	2.8
CMP601 O2′	Glu324 OE1	2.6	2.8	2.6
CMP601 O2′	Tyr371 OH	3.7	3.4	3.2
Arg333 NH1	Gly323 O	2.9	2.7	3.2

(b) Hydrogen Bond Interactions of the Solvent Network within the A-Site

atom 1	atom 2	distance (Å)	
		(R_p)−RIα	(S_p)−RIα
Wat701 O	CMP401 O2P (S2P)[a]	2.7	3.2
Wat701 O	Thr207 OG1	2.6	2.7
Wat701 O	Pro208 O	2.5	2.6
Wat701 O	Ala210 N	3.3	3.5
Wat702 O	CMP401 N6	2.6	2.6
Wat702 O	CMP401 N7	2.7	2.8
Wat702 O	Thr190 OG1	2.6	3.0
Wat702 O	Asp258 OD2	2.5	2.6

[a] The atoms in the parentheses correspond to the (S_p)−RIα structure. [b] Both exocyclic atoms are oxygen in the cAMP−RIα structure.

contrast, in cAMP−RIα and (S_p)−RIα where an oxygen atom occupies this equatorial position, the distances between this atom and the same side-chain nitrogen atom of Arg209 are 3.2 and 3.1 Å, respectively. This difference, indicative of a strong versus a weak hygrogen bond, indicates that the interaction between the (R_p)-cAMPS analogue, and the A-site is much tighter at this position, even though the overall affinity of (R_p)-cAMPS is less than for cAMP. Almost every bond distance of direct contact between the PBC motif and the ligand is shorter in (R_p)−RIα than in the cAMP−RIα and (S_p)−RIα structures. This is not true for the B-site of the (R_p)−RIα structure. In fact, the Arg333 in B-site has a shorter bond distances in the (S_p)−RIα. All of the direct or water-bridged interactions between the ligand and protein are summarized in Table 3. Another significant difference of the PBC motif in the (R_p)−, (S_p)−, and cAMP−RIα structures appears on the peptide segments that surround the invariant residues, Arg209/Arg333. Figure 4a shows that the backbone conformations of the fragment from residue 206 to residue 215 in domain A are slightly different in the three structures. The corresponding fragment 328−337 in domain B shows the largest conformational change in these structures, as shown in Figure 4b. The relative positions and orientations of the three ligands are basically the same when (R_p)- and (S_p)-analogues and cAMP are superimposed (Figures 4 and 5). They adopt a syn conformation with the adenine rings pointing toward the solvent-exposed interface. The adenine rings of the three ligands show very little difference when the structures are superimposed.

Two structural water molecules can be observed within the cAMP-binding pocket of domain A in the (R_p)−RIα and (S_p)−RIα structures (Figure 5a). Wat701 interacts with the phosphate group of the ligand but also is hydrogen-bonded to the protein by forming contacts to the main chain carboxyl atom of Pro208, to the backbone amide of Ala210, and to the side-chain hydroxyl group of Thr207. This water molecule, with a low *B*-factor of 26 Å^2, occupies a highly conserved position when the structures of (R_p)−RIα, (S_p)−RIα, Δ(1−111) RIIβ (*21*), and even the CAP protein (*34*) are superimposed (Figure 5b). The low resolution of the previous RIα structure did not allow for visualization of solvent molecules. Another water molecule (Wat702) is hydrogen-bonded to the N6 and N7 nitrogen atoms of the adenine ring. Wat702 also interacts with the OG1 atom of Thr190 from β5 of domain A and with the OD2 atom of Asp258 located on helix A of domain B. Thus the A-site cAMP can makes contact with helix A of domain B through this solvent molecule. Asp258, in turn, hydrogen bonds to Arg241, which interacts with the conserved glutamate in the PBC. This residue, Glu200 in domain A, hydrogen bonds to the 3′OH of the ribose moiety of cAMP bound to site A. Thus there is an extended network of interactions that link domain B to the cAMP binding site in domain A. A similar water molecule (Wat509) was found in the RIIβ structure, as shown in Figure 5b. These water-mediated contacts are

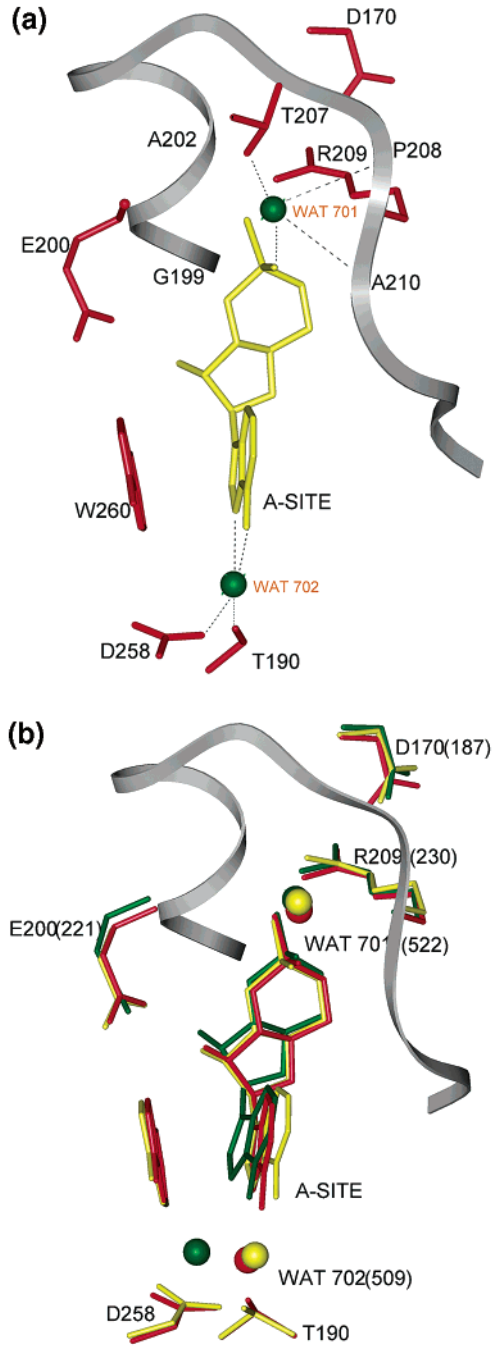

FIGURE 5: Solvent molecules in cAMP binding site A. Panel a shows two structural solvent molecules in the A-site pocket of (R_p)−RIα. The water atoms are shown in green. The water-bridged hydrogen bonds are indicated by dashed lines. The PBC motif (side chain in red) and ligand (yellow) are also shown. Panel b shows the PBC motif, ligand, and structural water atoms within A-site of (R_p)−RIα superimposed with those of (S_p)−RIα and cAMP−RIIβ. (R_p)−RIα is shown in red, (S_p)−RIα in yellow, and cAMP−RIIβ in dark green. The residues in parentheses correspond to the cAMP−RIIβ.

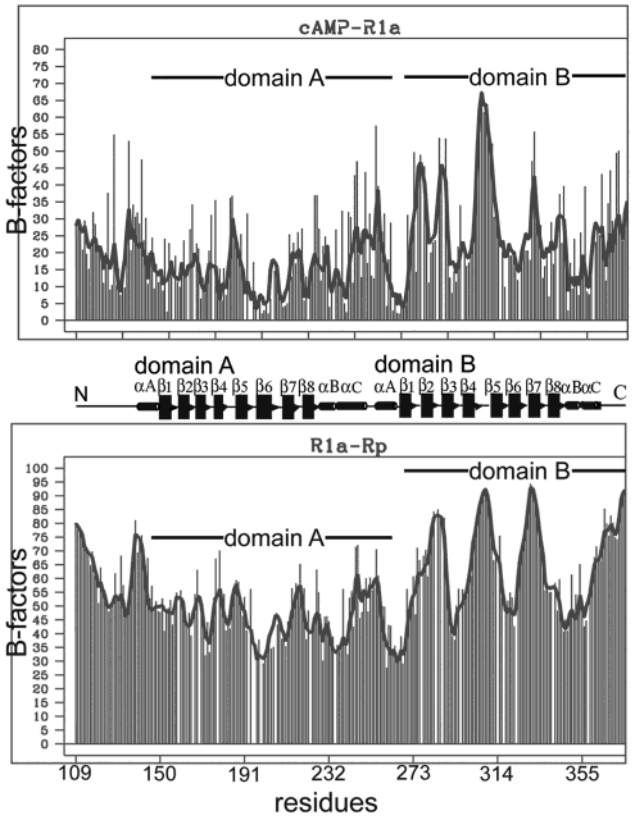

FIGURE 6: *B*-factor plots of (R_p)−RIα compared to cAMP−RIα. Comparison of the plots shows that the average *B*-factors in domain B are higher overall compared to domain A in (R_p)−RIα, while both domain A and domain B have the similar low *B*-factors in cAMP−RIα. *X*-axes correspond to the residue numbers, while *Y*-axes correspond to the *B*-factor value scale. Domain A contains residues 143−260; domain B contains residues 261−376. The corresponding secondary structural elements for Δ(1−91) RIα are also shown.

summarized in Table 3, section b. There are no structural solvent molecules found in the cAMP binding pocket of domain B.

Flexibility of Domain B. The regulatory subunits of PKA contain two tandem homologous cAMP binding domains, A and B. When occupied by cAMP, both domain A and domain B show similar stability, as indicated by their relatively similar and low *B*-factor values from the crystal structures of cAMP-bound RIα and RIIβ (*20*, *21*). The (S_p)−RIα structure is similar. A remarkable feature of the (R_p)−RIα structure is that the (R_p)-cAMPS ligand in the B-site, together with the entire domain B, appears to be much more dynamic relative to the A-site ligand and domain A. The plot of the *B*-factors in the refined (R_p)−RIα structure is shown in Figure 6. All peaks with high temperature factors can be attributed to loop regions located on the molecular surface. For example, the first peak corresponds to the surface loop (residues 135−143) connecting helix X_N and helix A. Figure 6 also shows that domain B is probably more flexible than domain A as indicated by the higher *B*-factors. This difference between domain A and domain B is not seen for the (S_p)−RIα structure or for cAMP−RIα or cAMP−RIIβ. The *B*-factor value of the A-site ligand is 34 Å^2 with a mean value of 47 Å^2 for the domain A (residues 143−260) in the (R_p)−RIα structure, while those of the B-site ligand and the domain B (261−376) are 65 and 63 Å^2, respectively.

DISCUSSION

There are two stable conformational states in vivo for the regulatory subunit of PKA: the dissociated cAMP-bound conformation (B-form), where cAMP occupies all four binding sites of the R dimer, and the cAMP-free holoenzyme conformation (H-form), where the cAMP-free protein forms an inactive holoenzyme complex by binding to the C-subunit.

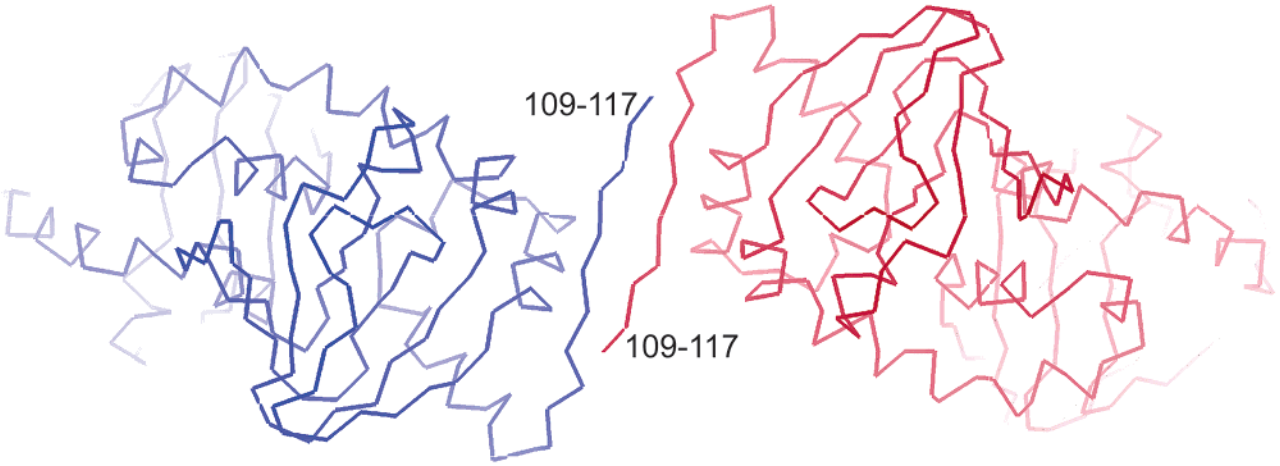

FIGURE 7: Crystal packing of Δ(1−91) RIα subunit. Two symmetry-related molecules form an intermolecular β-sheet by the N-terminal segment (109−117).

The allosteric binding of cAMP induces the R-subunit to shift from the H-form to the B-form. The molecular architectures of the cAMP bound conformations for RIα and RIIβ have been described on the basis of their crystal structures. Many biochemical lines of evidence, including the recent crystal structure of cAMP-free domain B of RIα (*35*) and H/D exchange studies coupled with mass spectrometry (*36*), indicate that the R-subunit undergoes a conformational change when it binds to the C-subunit. Surprisingly, major conformational changes do not appear to occur in the cAMP binding pocket, suggesting that the H-form and the B-form of the R-subunit do not display different global conformations. On the basis of the recent structure solution of a complex of C-subunit with domain A of RIα (Kim et al., unpublished results), domain A does assume a novel conformation when C is bound.

These studies do, however, identify a general allosteric pathway for communication between the PBC and the C binding surface involving helices A and B. On the basis of the increased dynamic properties described here, when (R_p)-cAMPS is bound the protein most likely cannot utilize the allosteric pathways that link cAMP binding to the release of C-subunit. The two events are uncoupled in the presence of (R_p)-cAMPS.

The (R_p)-cAMPS phosphothioate analogue functions as an antagonist, while cAMP and the (S_p)-cAMPS analogue cause the complex to dissociate when all binding sites are occupied. It was still in question whether the (R_p)-cAMPS binding would be sufficient to stabilize a different conformation (H-form) of the R-subunit even in the absence of the C-subunit, based on previous studies (*27*). Here the crystal structures of RIα complexed with (R_p)-cAMPS and (S_p)-cAMPS phosphothioate analogues, as well as the reported cAMP−RIα structure, show a similar overall molecular architecture (Figure 3). The largest rms deviation among the three structures is only 0.51 Å. These structures also share the same secondary structure patterns. The local conformations of the cAMP binding pockets are also similar, although some small changes occur in the segments around the two invariant arginine residues. These observations demonstrate that the RIα subunit exists in a cAMP-bound conformation even when bound to the cAMP antagonist, (R_p)-cAMPS, even though the increased dynamics suggests that ensembles will be present when (R_p)-cAMPS is bound. In the absence of C-subunit, (R_p)-cAMPS phosphothioate analogue is not sufficient to cause the R-subunit to switch from one conformation to the other.

The contact features of each cAMP binding site are similar to each other in (R_p)−RIα, (S_p)−RIα and cAMP−RIα structures. The phosphate group and the ribose ring are buried within the center of the β-barrel and make direct contacts with several highly conserved or invariant amino acid residues, as summarized in Table 3. When the (R_p)-cAMPS analogue occupies both binding sites in domains A and B, it makes a tighter interaction within the A-site than cAMP and the (S_p)-cAMPS analogue. For example, the bond distance between the equatorial sulfur atom (S1P) of (R_p)-cAMPS and the Arg209 side chain NE1 atom is shorter (2.6 Å) relative to the 3.2 Å on cAMP−RIα and 3.1 Å on (S_p)−RIα structures. Chemical studies indicate that the negative charge will reside on the sulfur in the (R_p)- or (S_p)-cAMPS phosphothioate analogues, while there will be significant resonance of electrons between the two exocyclic oxygens in cAMP (*27*). Obviously, the electrostatic contact between this negatively charged sulfur and the positively charged guanidinium side chain of Arg209 enhances the bond strength, behaving as a salt bond. There are weak hydrogen bonds between the equatorial oxygen and the Arg209 side chain in the cAMP−RIα and (S_p)−RIα structures. Surprisingly, the (R_p)-cAMPS analogue does not show this strong hydrogen bond in the B-site. The peptides around Arg209 in site A and Arg333 in site B show some conformational changes when the PBC motifs bound to the cAMP analogues are compared (Figure 4a,b). The fragment around Arg209 (residues 206−215) shows a slight difference, while the fragment 328−337 in site B shows a larger conformational change. It suggests that these peptide fragments will undergo conformational changes when binding to the cAMP analogues, especially on domain B.

Numerous solvent molecules can be observed within the A/B domain interfacial crevice, as mentioned above. This solvent-molecule network can access cAMP bound to site A. Two water molecules, Wat701 and Wat702 are located in the cAMP-binding pocket of domain A and form an extensive H-bond network with both ligand and the protein (Table 3, section b) in the (R_p)−RIα and (S_p)−RIα structures.

The Wat701-bridged H-bond network, which is close to the phosphate group, might effect the interaction between the cAMP ligand and the protein, helping to stabilize the ligand binding and also the water itself. Wat702 locates in the rim of the cAMP binding pocket of domain A. Through this water molecule, the cAMP adenine ring can make contact with both domain A and domain B of the RIα subunit.

The *B*-factor plot (Figure 6) indicates that the (R_p)-cAMPS analogue in B-site, together with the domain B, is significantly more flexible relative to A-site ligand and the domain A in the (R_p)−RIα structure. However, cAMP and (S_p)-cAMPS binding do not induce a similar flexibility of B-site ligand and domain B, as evidenced by analysis of the *B*-factor values of (S_p)−RIα, cAMP−RIα, and also the cAMP-bound RIIβ structures. This flexibility of domain B in the (R_p)−RIα structure can thus be attributed to the (R_p)-cAMPS binding to the protein. Many previous studies have indicated that the A-site is masked in the holoenzyme so that cAMP binds first to B-site of each regulatory monomer. This triggers a conformational change in the B-site, which serves as a "signal" that allows cAMP to bind to the A-site, then causing holoenzyme dissociation (*18*). An electrostatic network between the A-site and the B-site can be traced on the basis of the crystal structure of the RIα subunit. Initially, the B-site ligand interacts with Arg333. This invariant arginine forms a hydrogen bond with Glu289. Lys347, Glu270, Arg352, Lys240, Asp267, Arg241, and Glu200 then constitute a charge relay pathway leading from site B to site A where Glu200 binds directly to the ribose ring of cAMP bound to the A-site. This network of interactions, mostly electrostatic, is likely to be essential for the cooperative communication between domain A and domain B. In the case of the (R_p)-cAMPS analogue, it is the negatively charged sulfur that makes contact with Arg333. On the basis of the above discussions, some conformational changes within each cAMP binding site, together with the flexibility of the B-site ligand and domain B, provide a possible interpretation for why the (R_p)-cAMPS phosphothioate analogue functions as a competitive antagonist of cAMP. These differences most likely block the allosteric "signal" that allows domain B to communicate with domain A, thereby preventing the dissociation of holoenzyme. When (R_p)-cAMPS is bound, domain B can no longer effectively communicate with domain A. This communication network between the two domains is disrupted. This must be mediated primarily by an electrostatic effect where (R_p)-cAMPS is significantly different from cAMP.

Owing to the higher resolution X-ray data for (R_p)−RIα and (S_p)−RIα crystals, four more amino acid residues are included in the N-terminus of the newly refined structures. The N-terminal fragment (109−117) interacts with the same segment of a symmetry-related molecule, making an intermolecular antiparallel β-sheet, which forms an R homodimer by packing two monomers together (Figure 7). The crystal structure of an Apo A-domain mutant of RIα (residues 94−244) also demonstrates that the N-terminal segment shares the same packing pattern to form an intermolecular β-sheet, although the overall crystal packing is different (Akamine et al., unpublished results). It may imply that the Δ(1−91) deletion mutant of RIα can form a homodimer by its N-terminal linker region even without the dimerization domain.

ACKNOWLEDGMENT

We thank Wolfgang Dostmann for thoughtful discussions. We thank the staff at SSRL for help with data collection. Thanks to Kathy Ng for help with the manuscript preparation.

REFERENCES

1. Mitra, S., Zubay, G., and Landy, A. (1975) Evidence for the preferential binding of the catabolite gene activator protein (CAP) to DNA containing the *lac* promoter. *Biochem. Biophys. Res. Commun. 67*, 857−863.
2. Walsh, D. A., Perkins, J. P., and Krebs, E. G. (1968) An adenosine 3′,5′-monophosphate-dependent protein kinase from rabbit skeletal muscle. *J. Biol. Chem. 243*, 3763−3765.
3. Taylor, S. S., Buechler, J. A., and Yonemoto, W. (1990) cAMP-dependent protein kinase: framework for a diverse family of regulatory enzymes. *Annu. Rev. Biochem. 59*, 971−1005.
4. Ludwig, J., Margalit, T., Eismann, E., Lancet, D., and Kaupp, U. B. (1990) Primary structure of cAMP−gated channel from bovine olfactory epithelium. *FEBS Lett. 270*, 24−29.
5. de Rooij, J., Zwartkruis, F. J., Verheijen, M. H., Cool, R. H., Nijman, S. M., Wittinghofer, A., and Bos, J. L. (1998) Epac is a Rap1 guanine-nucleotide-exchange factor directly activated by cyclic AMP. *Nature 396*, 474−477.
6. Kawasaki, H., Springett, G. M., Mochizuki, N., Toki, S., Nakaya, M., Matsuda, M., Housman, D. E., and Graybiel, A. M. (1992) A family of cAMP-binding proteins that directly activate Rap1. *Science 282*, 2275−2279.
7. Døskeland, S. O., Maronde, E., and Gjertsen, B. T. (1993) The genetic subtypes of cAMP-dependent protein kinase − Functionally different or redundant? *Biochim. Biophys. Acta 1178*, 249−258.
8. Francis, S. H., and Corbin, J. D. (1999) Cyclic nucleotide-dependent protein kinases: intracellular receptors for cAMP and cGMP action. *Crit. Rev. Clin. Lab. Sci. 36*, 275−328.
9. Scott, J. D. (1991) Cyclic nucleotide-dependent protein kinases. *Pharmacol. Ther. 50*, 123−145.
10. Titani, K., Sasagawa, T., Ericsson, L. H., Kumar, S., Smith, S. B., Krebs, E. G., and Walsh, K. A. (1984) Amino acid sequence of the regulatory subunit of bovine type I adenosine cyclic 3′,5′-phosphate dependent protein kinase. *Biochemistry 23*, 4193−4199.
11. Øgreid, D., Ekanger, R., Suva, R. H., Miller, J. P., and Døskeland, S. O. (1989) Comparison of the two classes of binding sites (A and B) of type I and type II cyclic-AMP-dependent protein kinases by using cyclic nucleotide analogs. *Eur. J. Biochem. 181*, 19−31.
12. Rannels, S. R., and Corbin, J. D. (1981) Studies on the function of the two intrachain cAMP binding sites of protein kinase. *J. Biol. Chem. 256*, 7871−7876.
13. Døskeland, S. O., Øgreid, D., Ekanger, R., Sturm, P. A., Miller, J. P., and Suva, R. H. (1983) Mapping of the two intrachain cyclic nucleotide binding sites of adenosine cyclic 3′,5′-phosphate dependent protein kinase I. *Biochemistry 22*, 1094−1101.
14. Ringheim, G. E., Saraswat, L. D., Bubis, J., and Taylor, S. S. (1988) Deletion of cAMP-binding site B in the regulatory subunit of cAMP-dependent protein kinase alters the photoaffinity labeling of site A. *J. Biol. Chem. 263*, 18247−18252.
15. Neitzel, J. J., Dostmann, W. R. G., and Taylor, S. S. (1991) Role of MgATP in the activation and reassociation of cAMP-dependent protein kinase I: consequences of replacing the essential arginine in cAMP binding site A. *Biochemistry 30*, 733−739.
16. Herberg, F. W., Taylor, S. S., and Dostmann, W. R. G. (1996) Active site mutations define the pathway for the cooperative activation of cAMP-dependent protein kinase. *Biochemistry 35*, 2934−2942.
17. Zorn, M., Fladmark, K., Øgreid, D., Jastorff, B., Døskeland, S. O., and Dostmann, W. R. G. (1995) Ala335 is essential for high-affinity cAMP-binding of both sites A and B of cAMP-dependent protein kinase type I. *FEBS Lett 362*, 291−294.
18. Øgreid, D., and Døskeland, S. O. (1982) Activation of protein kinase isoenzymes under near physiological conditions. Evidence that both types (A and B) of cAMP binding sites are involved in

the activation of protein kinase by cAMP and 8-N3-cAMP. *FEBS Lett 150*, 161−166.
19. Bubis, J., and Taylor, S. S. (1987) Correlation of photolabeling with occupancy of cAMP binding sites in the regulatory subunit of cAMP-dependent protein kinase I. *Biochemistry 26*, 3478−3486.
20. Su, Y., Dostmann, W. R. G., Herberg, F. W., Durick, K., Xuong, N., Eyck, L. T., Taylor, S. S., and Varughese, K. L. (1995) Regulatory subunit of protein kinase A: structure of deletion mutant with cAMP binding domains. *Science 269*, 807−813.
21. Diller, T. C., Madhusudan, Xuong, N., and Taylor, S. S. (2001) Molecular basis for regulatory subunit diversity in cAMP-dependent protein kinase: crystal structure of the type II beta regulatory subunit. *Structure 9*, 73−82.
22. Kang, G., Joseph, J. W., Chepurny, O. G., Monaco, M., Wheeler, M. B., Bos, J. L., Schwede, F., Genieser, H. G., and Holz, G. G. (2003) Epac-selective cAMP analog 8-pCPT-2′−O-Me-cAMP as a stimulus for Ca2+-induced Ca2+ release and exocytosis in pancreatic beta-cells. *J. Biol. Chem. 278*, 8279−8285.
23. Schwede, F., Maronde, E., Genieser, H. G., and Jastorff, B. (2000) Cyclic nucleotide analogs as biochemical tools and prospective drugs. *Pharmacol. Ther. 87*, 199−226.
24. Rothermel, J. D., and Botelho, L. H. P. (1988) A mechanistic and kinetic analysis of the interactions of the diastereoisomers of adenosine 3′,5′-(cyclic)phosphorothioate with purified cyclic AMP-dependent protein kinase. *Biochem. J. 251*, 757−762.
25. DeWit, R. J. W., Hekstra, D., Jastorff, B., Stec, W. J., Baraniak, J., Driel, R. V., and van Haastert, P. J. M. (1984) Inhibitory action of certain cyclophosphate derivatives of cAMP on cAMP-dependent protein kinases. *Eur. J. Biochem. 152*, 255−260.
26. Dostmann, W. R. G., Taylor, S. S., Genieser, H. G., Jastorff, B., Døskeland, S. O., and Øgreid, D. (1990) Probing the cyclic nucleotide binding sites of cAMP-dependent protein kinases I and II with analogs of adenosine 3′,5′-cyclic phosphorothioates. *J. Biol. Chem. 265*, 10484−10491.
27. Dostmann, W. R. G. (1995) (RP)-cAMPS inhibits the cAMP-dependent protein kinase by blocking the cAMP-induced conformational transition. *FEBS Lett. 375*, 231−234.
28. Dostmann, W. R. G., and Taylor, S. S. (1991) Identifying the molecular switches that determine whether (Rp)-cAMPS functions as an antagonist or an agonist in the activation of cAMP-dependent protein kinase I. *Biochemistry 30*, 8710−8716.
29. Saraswat, L. D., Filutowics, M., and Taylor, S. S. (1988) Expression and mutagenesis of the regulatory subunit of cAMP-dependent protein kinase in *Escherichia coli*. *Method Enzymol. 159*, 325−336.
30. Otwinowski, Z., and Minor, W. (1997) Processing of X-ray data collected in oscillation mode. *Method Enzymol. 276*, 307−326.
31. Brunger, A. T., Adams, P. D., and Clore, G. M. (1998) Crystallography and NMR system: A new software suite for macromolecular structure determination. *Acta Crystallogr. D54*, 905−921.
32. Roussel, A., and Cambillau, C. (1991) *Turbo-Frodo, Silicon Graphics partner geometry dictionary*, Silicon Graphics Inc., Mountain View, CA.
33. Morris, A. L., MacArthur, M. W., Hutchinson, E. G., and Thornton, J. M. (1992) Stereochemical quality of protein structure coordinates. *Proteins: Struct., Funct., Genet. 12*, 345−364.
34. Weber, I. T., and Steitz, T. A. (1987) Structure of a complex of catabolite gene activator protein and cyclic AMP refined at 2.5 Å resolution. *J. Mol. Biol. 198*, 311−326.
35. Wu, J., Brown, S., Xuong, N. H., Taylor, S. S. RIα subunit of PKA: A cAMP-free structure reveals a hydrophobic capping mechanism for docking cAMP into site B. *Structure*, in press.
36. Anand, G. S., Hughes, C. A., Jones, J. M., Taylor, S. S., and Komives, E. A. (2002) Amide H/2H exchange reveals communication between the cAMP and catalytic subunit-binding sites in the R(I)alpha subunit of protein kinase A. *J. Mol Biol. 323*, 377−386.

BI0302503